NASA TR R-41

NATIONAL AERONAUTICS AND SPACE ADMINISTRATION

TECHNICAL REPORT
R-41

NORMAL COMPONENT OF INDUCED VELOCITY FOR ENTIRE FIELD OF A UNIFORMLY LOADED LIFTING ROTOR WITH HIGHLY SWEPT WAKE AS DETERMINED BY ELECTROMAGNETIC ANALOG

By WALTER CASTLES, JR., HOWARD L. DURHAM, JR.,
and JIRAIR KEVORKIAN

1959

For sale by the Superintendent of Documents, U.S. Government Printing Office, Washington 25, D.C. Yearly subscription, $10; foreign, $13; single copy price varies according to size --------- Price 40 cents

TECHNICAL REPORT R-41

NORMAL COMPONENT OF INDUCED VELOCITY FOR ENTIRE FIELD OF A UNIFORMLY LOADED LIFTING ROTOR WITH HIGHLY SWEPT WAKE AS DETERMINED BY ELECTROMAGNETIC ANALOG

By WALTER CASTLES, JR., HOWARD L. DURHAM, JR., and JIRAIR KEVORKIAN

Georgia Institute of Technology

TECHNICAL REPORT R-41

NORMAL COMPONENT OF INDUCED VELOCITY FOR ENTIRE FIELD OF A UNIFORMLY LOADED LIFTING ROTOR WITH HIGHLY SWEPT WAKE AS DETERMINED BY ELECTROMAGNETIC ANALOG[1]

By Walter Castles, Jr., Howard L. Durham, Jr., and Jirair Kevorkian

SUMMARY

Values of the nondimensional normal component of induced velocity throughout the flow field of a uniformly loaded lifting rotor operating in the upper half of the helicopter speed range are presented in the form of graphs and tables. The tabulated data are for rectangular grids of points located in azimuth planes situated at 30° increments of azimuth angle. The grids extend a distance of 4 rotor radii in both the vertical and radial directions. Values at points in the rotor plane were computed by means of the Biot-Savart relation using the assumption that the wake-vortex distribution consisted of a uniform, semi-infinite, elliptic cylinder. Values at points not in the rotor plane were obtained experimentally by measurements of the field strength about an electromagnetic-analog model of the wake-vortex system.

Comparisons of computed and experimental analog values for the normal component of induced velocity both in the plane of the rotor and in the lateral plane perpendicular to the rotor plane are presented. The agreement between the computed and experimental analog values indicates that the latter are sufficiently accurate for engineering purposes.

The results should be useful for estimating the induced velocity distribution about lifting rotors in general and for synthesizing the distributions over the rotor disk for the case of any specified nonuniform loading.

INTRODUCTION

In order to determine the performance and air load distribution of a lifting rotor, it is necessary to know the induced flow field in the vicinity of the rotor, the component of velocity normal to the plane of the rotor being of particular interest.

To make rotor-flow-field computations mathematically tractable, it is usual to approximate the actual wake-vortex system by one having regular geometric properties. In general, however, for even the simplest of wake geometries the calculations are tedious and prohibitively lengthy unless high-speed computing facilities are available. Alternatively, there is an approach to the problem making use of the perfect analogy between the induced flow field associated with a vortex filament in a perfect fluid and the magnetic field in space associated with a current-carrying wire. Thus it is possible to construct an electromagnetic analog in the form of a wire model of a given vortex configuration. Point measurements of magnetic-field strength in the associated magnetic field then afford a description of the analogous induced velocity in the fluid velocity field, as shown in reference 1.

The principal objective of the present paper is to present in the form of tables and graphs the experimental values for the nondimensional normal component of induced velocity which were obtained by means of an electromagnetic-analog model of the wake from a rotor operating in the upper half of the flight speed range. The method employed was in many respects similar to the procedures described in references 1 and 2. Surveys were made of the normal component of induced velocity in several azimuth planes perpendicular to the plane of the rotor beginning with the longitudinal plane of symmetry and proceeding in 30° increments of azimuth angle.

Another objective is to supplement and extend the results of references 3 and 4 by presenting

[1] Supersedes NACA Technical Note 4238 by Walter Castles, Jr., Howard L. Durham, Jr., and Jirair Kevorkian 1958

additional computed values, obtained by means of a digital computer, of the normal component of induced velocity in the rotor plane. This program was carried out along with the magnetic-analog measurements and afforded reliable check points for comparison of results. The computed data furnished values for the induced velocity at space points located such that physical interference between the pickup coil and wake model prevented field measurements and also at points near the model coils where the gradient of the local magnetic field was large.

The analysis presented herein concerns the flow field associated with a uniformly loaded lifting rotor and assumes that the wake-vortex system has the form of a uniform, semi-infinite, elliptic cylinder composed of a very large number of circular vortex ring elements arranged in such a way that the circulation per unit length of the vortex sheet is constant. This assumption implies that the induced flow associated with the vortex system is a potential flow and, as such, has a perfect magnetic analogy as pointed out by equations (2) and (3) of reference 1.

This investigation was conducted at the Georgia Institute of Technology under the sponsorship and with the financial assistance of the National Advisory Committee for Aeronautics.

SYMBOLS

a_1 coefficient of cosine term in Fourier series for blade flapping angle

MR output meter reading, db

m tangent of wake angle χ

P any point $P(X_o,Y_o,Z_o)$ in rotor flow field

R rotor radius

R_o radius of point P from $Z-$ or rotor axis

R_C,ψ,Z_C cylindrical coordinates of a point on the curve of intersection of plane $\psi=$Constant with wake-vortex cylinder

$r_o=R_o/R$

V velocity of helicopter along flight path

V_i normal component of induced velocity at P

v normal component of induced velocity at center of rotor plane

X,Y,Z coordinates of a wake-vortex sheet element as measured relative to the tip-path-plane axes

X_o,Y_o,Z_o coordinates of point P in rotor flow field

$z_o \quad Z_o/R$

α angle of attack of plane of zero feathering

α_v angle of attack of rotor plane, $\alpha-a_1$

θ azimuth angle of wake-vortex sheet element having length ds measured from negative $X-$ or upwind direction

$\lambda_v=(V \sin \alpha_v-v)/\Omega R$

$\mu_v=(V \cos \alpha_v)/\Omega R$

χ wake angle measured between negative $Z-$ or rotor axis and wake axis

ψ azimuth angle of point P measured from positive $X-$ or downwind direction

Ω angular velocity of rotor blades

Subscripts:

C curve of intersection formed by plane $\psi=$Constant with wake-vortex cylinder

N search-coil normalizing point for which computed velocity ratio was known

P point P

THEORETICAL ANALYSIS

Under the assumption that the wake-vortex distribution takes the form of a uniform, semi-infinite, elliptic cylinder, it was shown in reference 4 that the ratio of the normal component of induced velocity at any point P to that at the center of the rotor is given by

$$\left(\frac{V_i}{v}\right)_{r_o,\, m,\, z_o,\, \psi}=\frac{1}{2\pi}\int_0^{2\pi}\frac{A-B\sqrt{C}}{\sqrt{C}(\sqrt{C}-D)}\,d\theta \qquad (1)$$

where the wake geometry is given in figure 1 and

$$A=1+r_o\cos(\psi-\theta)$$

$$B=m\cos\theta/\sqrt{1+m^2}$$

$$C=1+r_o^2+z_o^2+2r_o\cos(\psi-\theta)$$

$$D=(z_o+mr_o\cos\psi+m\cos\theta)/\sqrt{1+m^2}$$

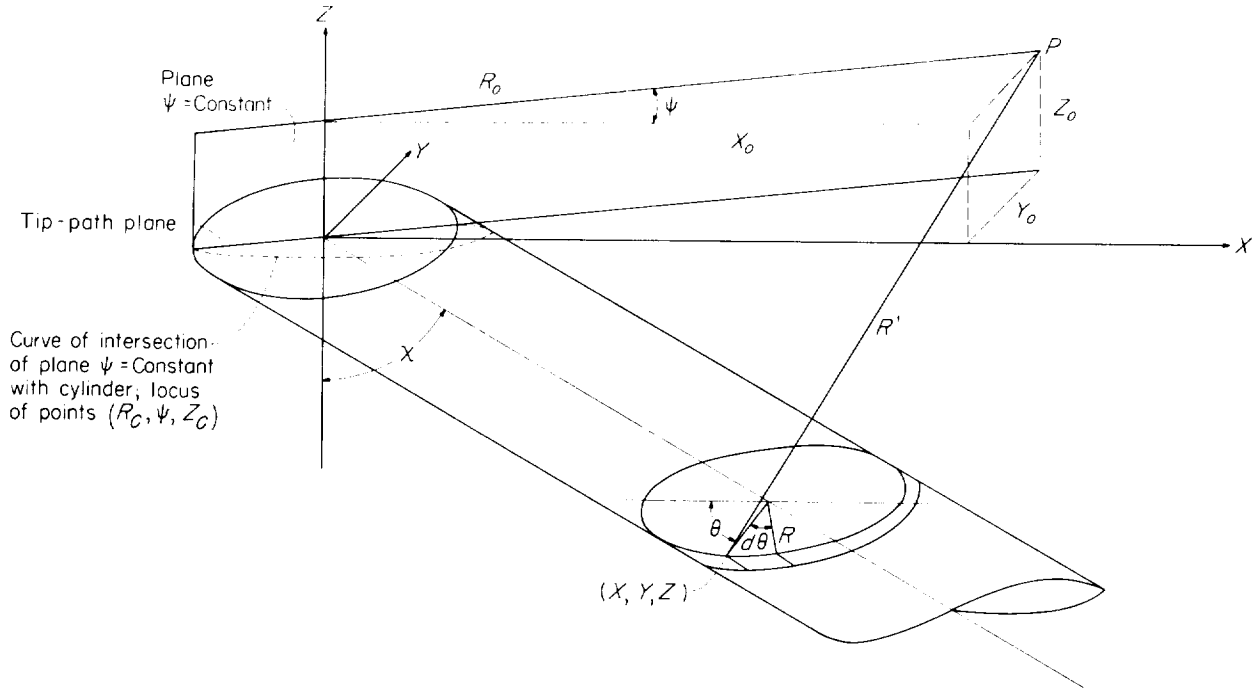

FIGURE 1.- Geometry of wake-vortex system.

The wake angle χ is connected with the resultant velocity components at the center of the rotor by the relation

$$\chi = \tan^{-1}(-\mu_r/\lambda_r) \tag{2}$$

It was desired to compute the nondimensional normal component of induced velocity in the rotor plane at points $P(r_o, \psi)$ for a wake geometry simulating the wake from a rotor operating in the upper half of the helicopter speed range. Since a wake angle $\chi = \tan^{-1} 10$ (84.29°) closely approximates the actual wake angle for a helicopter operating in the higher speed range, the values $z_o = 0$ and $m = 10$ were substituted into equation (1) which then became

$$\left(\frac{V_i}{V}\right)_{r_0,10,0,\psi} = \frac{1}{2\pi}\int_0^{2\pi} H \, d\theta \tag{3}$$

where H represents the integrand of equation (1) after the substitutions were made in the quantities A, B, C, and D above.

Numerical approximations to the integral of equation (3) were obtained for combinations of values of r_o and ψ by means of a digital computer programmed to use Simpson's rule with 120 equally spaced increments in θ. Except for a few points close to the wake boundary, this procedure yielded results correct to within ± 1 in the third decimal place as verified by check points previously computed by other methods.

EXPERIMENTAL PROCEDURE

The electrical systems employed in references 1 and 2 were broadly similar in that both included four basic components:

(1) The primary coil (wire model of vortex system)
(2) The secondary coil (search coil)
(3) The electronic voltmeter
(4) The power supply

The methods consisted essentially of measuring the voltage induced in the search coil by the magnetic field of the primary-coil current and converting the result into equivalent velocity.

In light of information gained from the reports mentioned above, certain fixed considerations emerge which affect the accuracy of the method and must be taken into account when designing an electromagnetic-analog system. These include:

(1) Extraneous magnetic fields
(2) Impure wave forms in the primary-coil circuit

(3) Induced effects in the primary-coil and search-coil leads
(4) Search-coil dimensions and calibration
(5) Primary-coil field distortion

An attempt was made in the present work to minimize inaccuracies arising from the above sources. The following sections describe each of the basic components of the magnetic-analog system used in this investigation.

PRIMARY FIELD COIL (WAKE MODEL)

The difficulties involved in attempting to construct a solid nonmagnetic cylinder in the shape of an elliptic cylinder upon which to wind the primary coil made it expedient to build up the wake model from a series of "lumped" coils wound on separate Plexiglas rings. The rings were mounted upon a heavy fiber base plate by means of individual Plexiglas bases so arranged that the line of centers made an angle of 84.29° (or $\tan^{-1} 10$) with the rotor plane axis. To minimize the field distortion due to lumped coils in the vicinity of the rotor plane, the assembly was divided into two principal sections. The first section (corresponding to the upper portion of the wake) consisted of 27 rings each bearing 1 turn of No. 17 gage copper wire. The second section was comprised of 18 rings each bearing 9 turns of wire and a final ring bearing two layers of 9 turns each. The coils were connected in series in such a manner that the input and return wires for each coil were juxtaposed and could be twisted. This arrangement, which for the multiturn coils involved a double winding, was necessary in order to minimize the external magnetic field induced by the current in the individual coil leads. The leads connecting the wake model to the power supply issued from the final coil at the end of the wake model and were also twisted. The wake coils had a mean diameter of 12 inches between wire centers and were so spaced that the average number of turns per unit wake length was the same in each section. It should be noted that the position of the rotor plane does not coincide with the plane of the end coil but is located approximately half a coil turn farther up the wake axis. The relative positioning of the coils conformed roughly to the actual spacing of the rotor-blade tip vortices in the wake of a three-bladed helicopter rotor operating at $\mu_r = 0.3$. The overall length of the assembly was 12 feet. Under operating conditions the "equivalent vortex" strength of the field coil was about 4 ampere turns per inch of wake length. The entire coil system was mounted on a wooden table of height and position such that the wake model was centered in its containing room. Figure 2 is a photograph of the model assembly.

SEARCH COIL

The nonlinearity of the primary-coil field and the fact that point measurements were desired made it necessary that the search-coil dimensions be small compared with those of the wake model. A mean diameter for the search coil amounting to about 3 percent of that for the field coils was adopted for the work reported herein, since a coil of such size could be built with little difficulty and would yield induced voltage measurements sufficiently accurate for engineering purposes. The search coil used had a diameter of about 0.35 inch to the center of the wire bundle which had a cross section in the form of a square approximately 0.09 inch on a side. The coil consisted of 1,000 turns of No. 40 gage copper wire wound on a Plexiglas form. The coil form was mounted on a Plexiglas support. A solid dielectric coaxial cable was used to connect the search coil to the amplifier in order to minimize the current induced in this section of the pickup circuit. The entire search-coil assembly together with its coaxial connector is shown in figure 2. The base of the search-coil support and also the top of the field-coil supporting table were scribed with straight lines spaced at increments of convenient fractions of the rotor radius in order to facilitate positioning of the search coil. For surveys in the various azimuth planes, wooden ramps having the shape of 30° or 60° triangles were used to position the search-coil assembly. Scribed lines were also included on the faces of these supports. The search-coil assembly is shown typically positioned relative to the wake model in figure 2. Figure 3 shows the search coil in detail.

The necessity for obtaining a separate calibration of the search-coil circuit was eliminated in the work of this report by normalizing the field-strength measurements to those obtained at several convenient space locations in the primary-coil field for which the values of the induced velocity are given in reference 4.

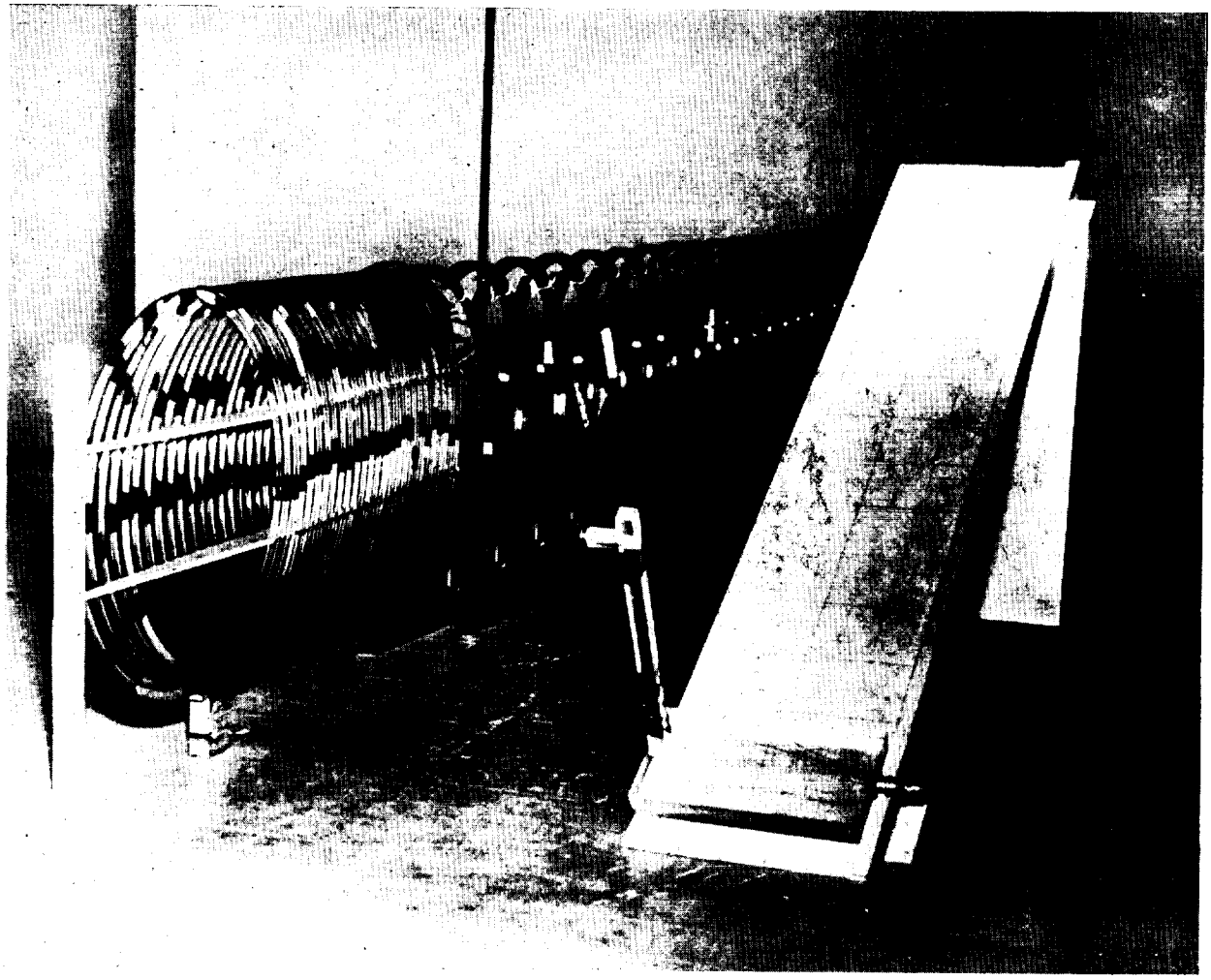

FIGURE 2.—Magnetic-analog model assembly simulating a wake angle of $\chi = \tan^{-1} 10 = 84.29°$.

AMPLIFIER AND OUTPUT METER

In addition to the search coil, the pickup circuit included a commercial standing wave indicator having a maximum sensitivity of 0.1 microvolt for full-scale meter deflection. The assembly consisted of an indicating meter, a high-gain 400-cycle fixed-frequency amplifier with a calibrated gain control covering a range of 60 decibels, and a narrow 400-cycle band-pass-filter network having a sharp cutoff at 400 $\pm$ 5 cycles per second. The integral electronically regulated internal power supply operated on 115 volts. The input impedance of the amplifier was 200,000 ohms and consequently it was desirable to test whether calibration factors in terms of the search-coil current were needed for the indicator readings. This was done by placing the search coil at various points of high and low field strength and taking meter readings with only the normal 200,000-ohm impedance in the amplifier input circuit. A set of ratios of the equivalent induced velocities was computed from these readings. The input impedance was then changed to approximately 5 megohms by means of a noninductive series resistor and the procedure was repeated. A comparison of the two sets of computed ratios showed no measurable differences. It was concluded that meter scale calibration was unnecessary. Figure 4 shows the amplifier-indicator unit which was located in a hallway removed from the field coil.

POWER SUPPLY

The power supply used for the wake model consisted of a 400-cycle aircraft inverter driven

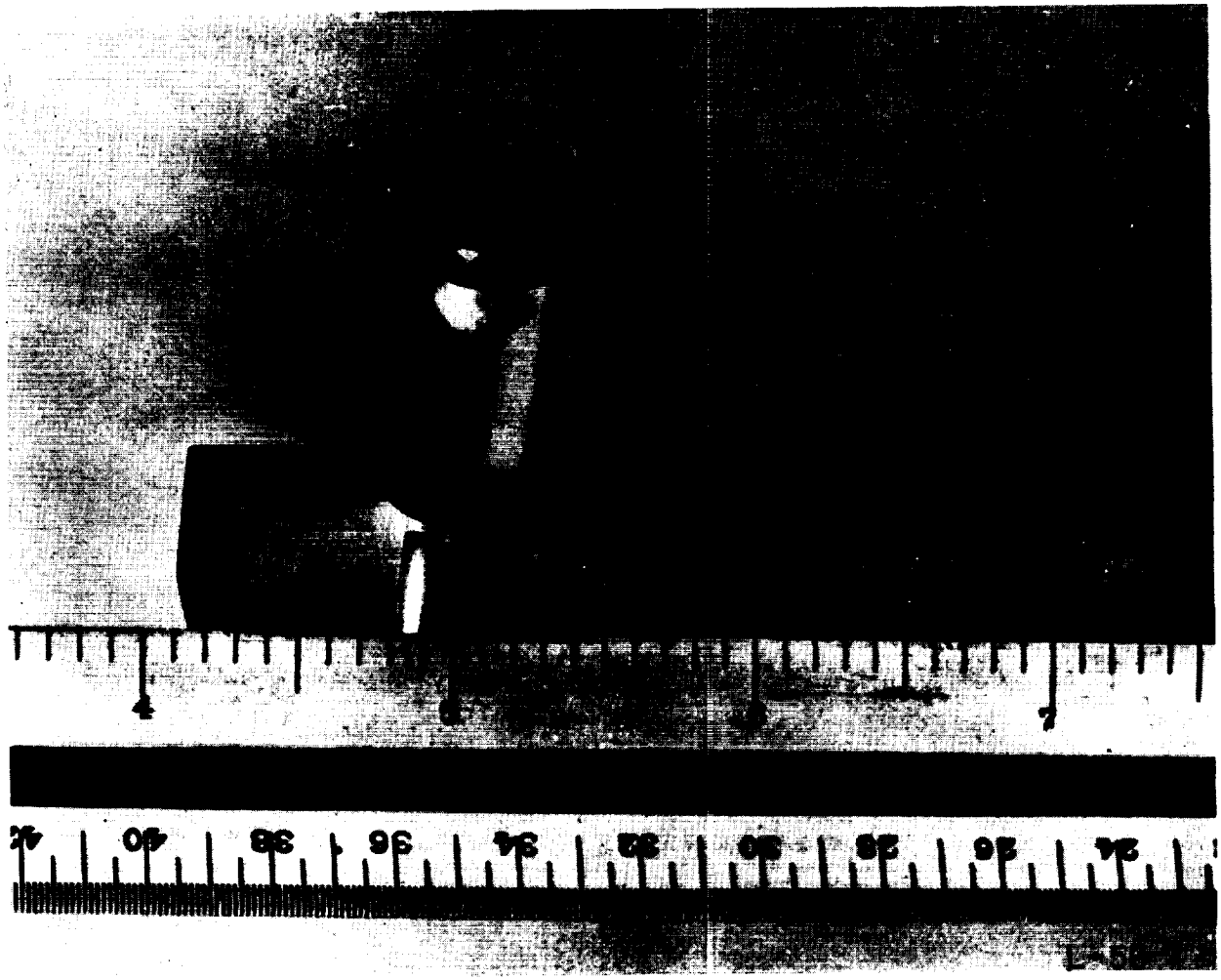

FIGURE 3. Details of search coil.

by a rectifier, the output voltage of which was stabilized by storage batteries. The inverter was connected to the primary magnet coil through a variable series resistor and through series capacitance. It was found that the frequency stability of the system was improved by adjusting the capacitance so that the resonant frequency of the wake-model coil circuit was slightly above the 400-cycle operating frequency. As monitoring devices the circuit included an ammeter and an electrically driven reed frequency meter which had been reworked so that the frequencies indicated by successive reeds differed by only 1 cps. Rough frequency control was obtained by means of inverter taps, and final frequency adjustment to the desired 400 cps was made by varying the load on the inverter through the series resistor. In order to use this frequency control system it was necessary to unbalance slightly the frequency-load-compensation circuit in the inverter. Figure 5 shows the power-supply assembly which was located in a separate room from those of the wake-model coil and amplifier.

FIELD-SURVEY PROCEDURE

In general, the wake-model coil circuit was allowed to operate for about 30 minutes in order to reach thermal equilibrium before any attempt was made to take measurements. After stable conditions were reached, the search coil was placed at a convenient normalizing point in the magnetic field for which the induced velocity ratio was known from the digital-computer calculations of reference 4 and the meter reading recorded. The

FIGURE 4.—Fixed-frequency amplifier and indicator unit.

coil was then moved to the successive survey positions and these readings recorded. The search-coil circuit was renormalized at frequent time intervals.

REDUCTION OF DATA

The meter readings recorded during the procedure described in the preceding section were converted into equivalent velocity ratios by the formula

$$\left|\left(\frac{V_i}{v}\right)_P\right| = \left(\frac{V_i}{v}\right)_N \left[\frac{\text{antilog } 0.1(MR)_P}{\text{antilog } 0.1(MR)_N}\right] \quad (4)$$

where V_i/v is the nondimensional normal component of induced velocity and P refers to the space point at which the measurement was made.

The sign (direction) associated with the left member of equation (4) was determined from considerations embracing the flow-field geometry and the trends of the experimental data being reduced. The results, as described in the next section, were obtained from faired plots of the experimentally determined induced velocity ratio V_i/v plotted against R_o/R for constant values of Z_o/R or, where necessary, against Z_o/R at constant values of R_o/R.

RESULTS

Tables 1(a) to 1(g) give the values of V_i/v as experimentally determined over the azimuth planes $\psi=0°$, 30°, 60°, 90°, 120°, 150°, and 180°. Because of the symmetry of the flow, tables 1(b) to 1(f) also hold for the azimuth planes $\psi=330°$, 300°, 270°, 240°, and 210°, respectively. In table 1(d) the values of V_i/v at points for which

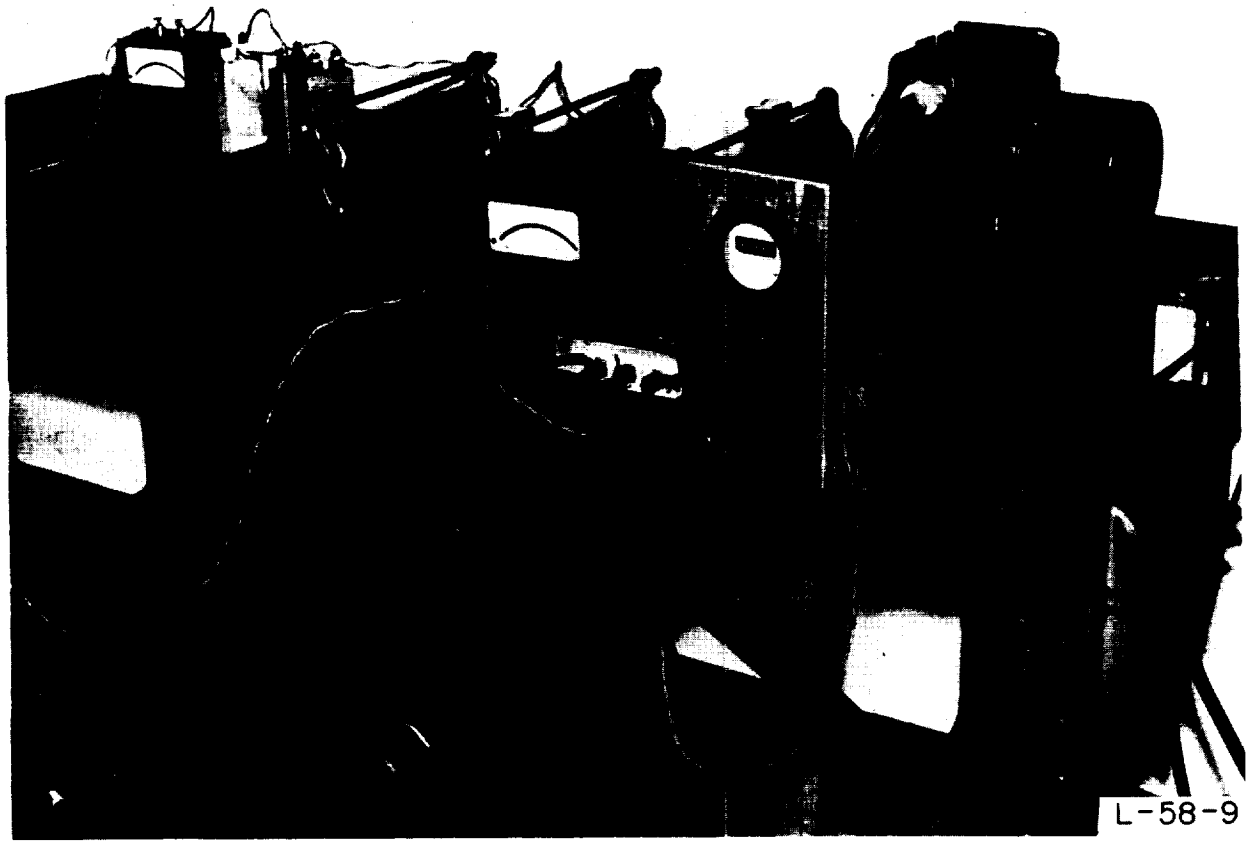

FIGURE 5. Power-supply assembly.

$0 \leqq R_c/R \leqq 2.8$ and $-2 \leqq Z_c/R \leqq 2$ were taken directly from the computed results obtained in reference 4. The measurements given in table 1 extend over a large enough region about the rotor plane so that the velocity distributions near a rotor with nonuniform loading may be calculated by superposition as in reference 5.

Table 2 lists the computed values for V_i/v in the rotor plane at azimuth angles $\psi = 0°$, 30°, 60°, 90°, 120°, 150°, and 180° extending radially to six rotor radii. Although the table contains some duplication of values previously listed, it was thought convenient in light of possible future application to collect the in-plane components together.

Figures 6(a) to 6(d) are plots of constant values of V_i/v in the various azimuth planes as interpolated from tables 1(a) to 1(g). In particular, figure 6(a) supplements the collection of similar plots given in reference 3, and figure 6(d) extends the ranges covered by its corresponding plot in reference 4. The dashed lines in each figure represent the curve of intersection formed by the azimuth plane and the wake vortex cylinder. Points on these dashed curves are given by the relation

$$\frac{Z_c}{R} = \cot \chi \left[-\frac{R_c}{R} \cos \psi \pm \sqrt{1 - \left(\frac{R_c}{R} \sin \psi \right)^2} \right] \quad (5)$$

where only negative values of Z_c are to be considered.

Figure 7 compares constant-value plots as obtained from the computed values of table 1(d)

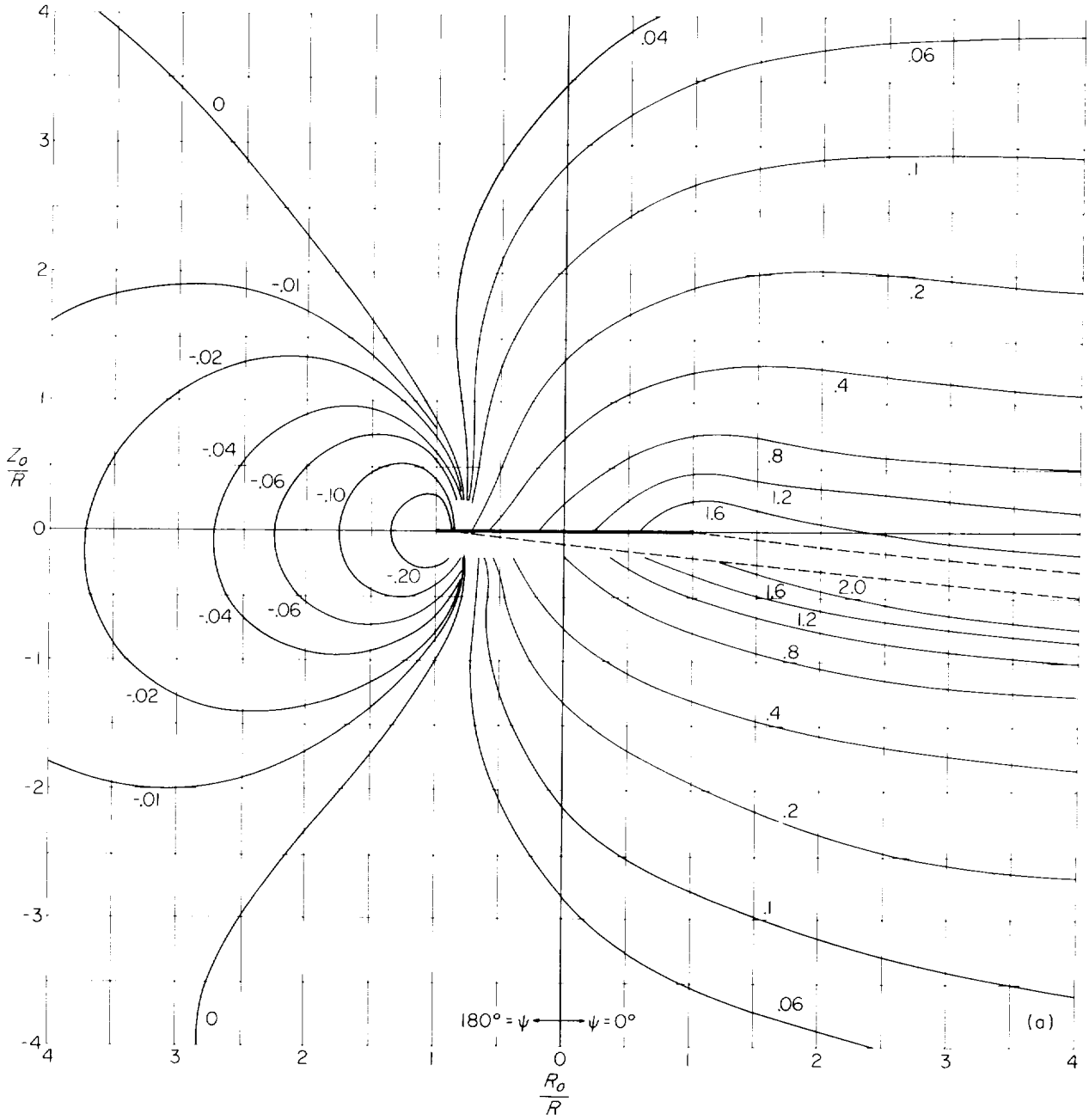

(a) Lines of constant values of V_i/v in longitudinal plane $\psi = 0°$ and 180°.

FIGURE 6.- Lines of constant values of nondimensional normal component of induced velocity V_i/v in each 30° azimuth plane for case of a wake angle $\chi = \tan^{-1} 10 = 84.29°$. Dashed lines represent curve of intersection formed by azimuth plane and wake-vortex cylinder.

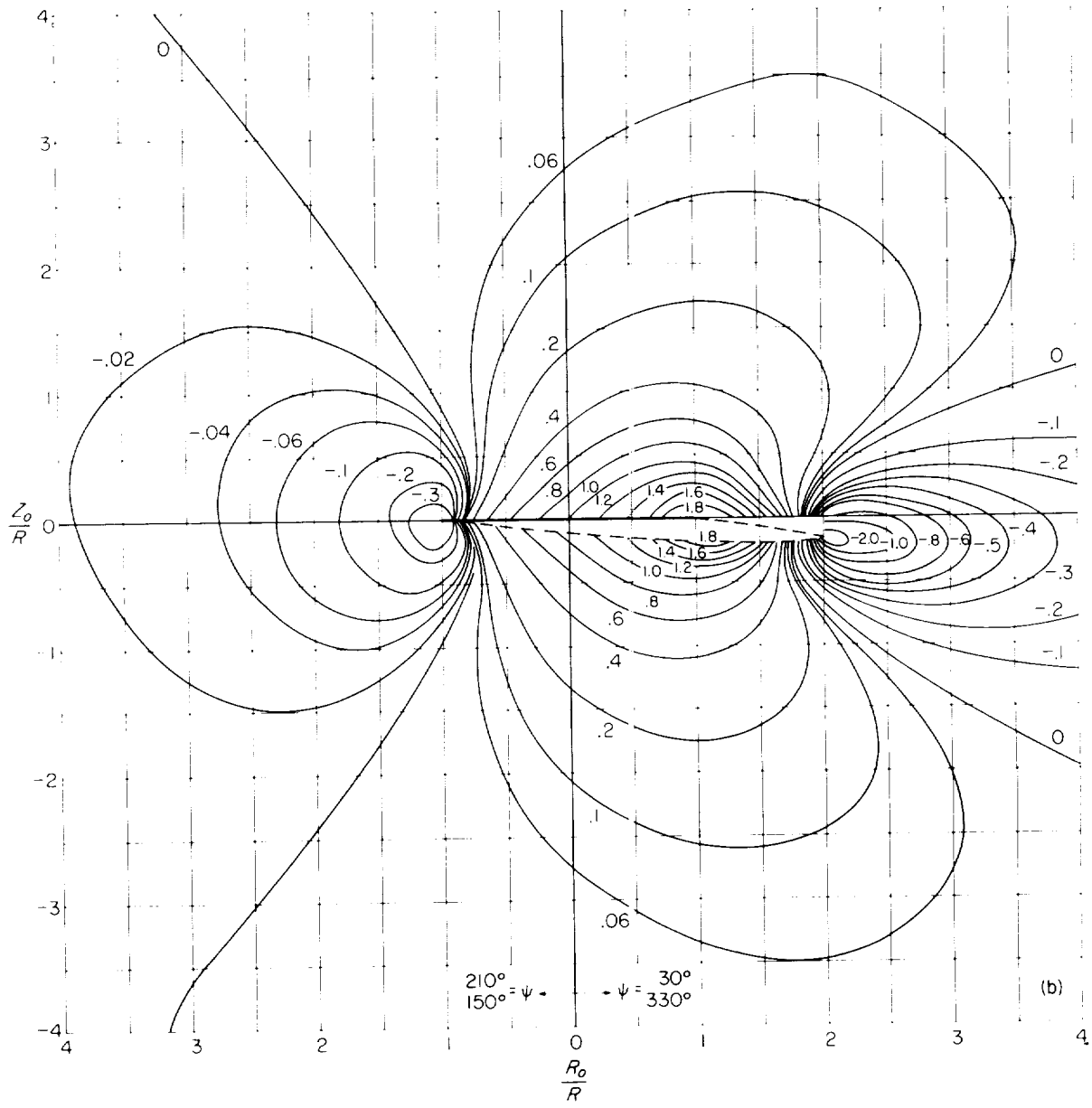

(b) Lines of constant values of V_r/v in azimuth planes $\psi = 30°$ and $210°$ and $\psi = 150°$ and $330°$.

FIGURE 6.— Continued.

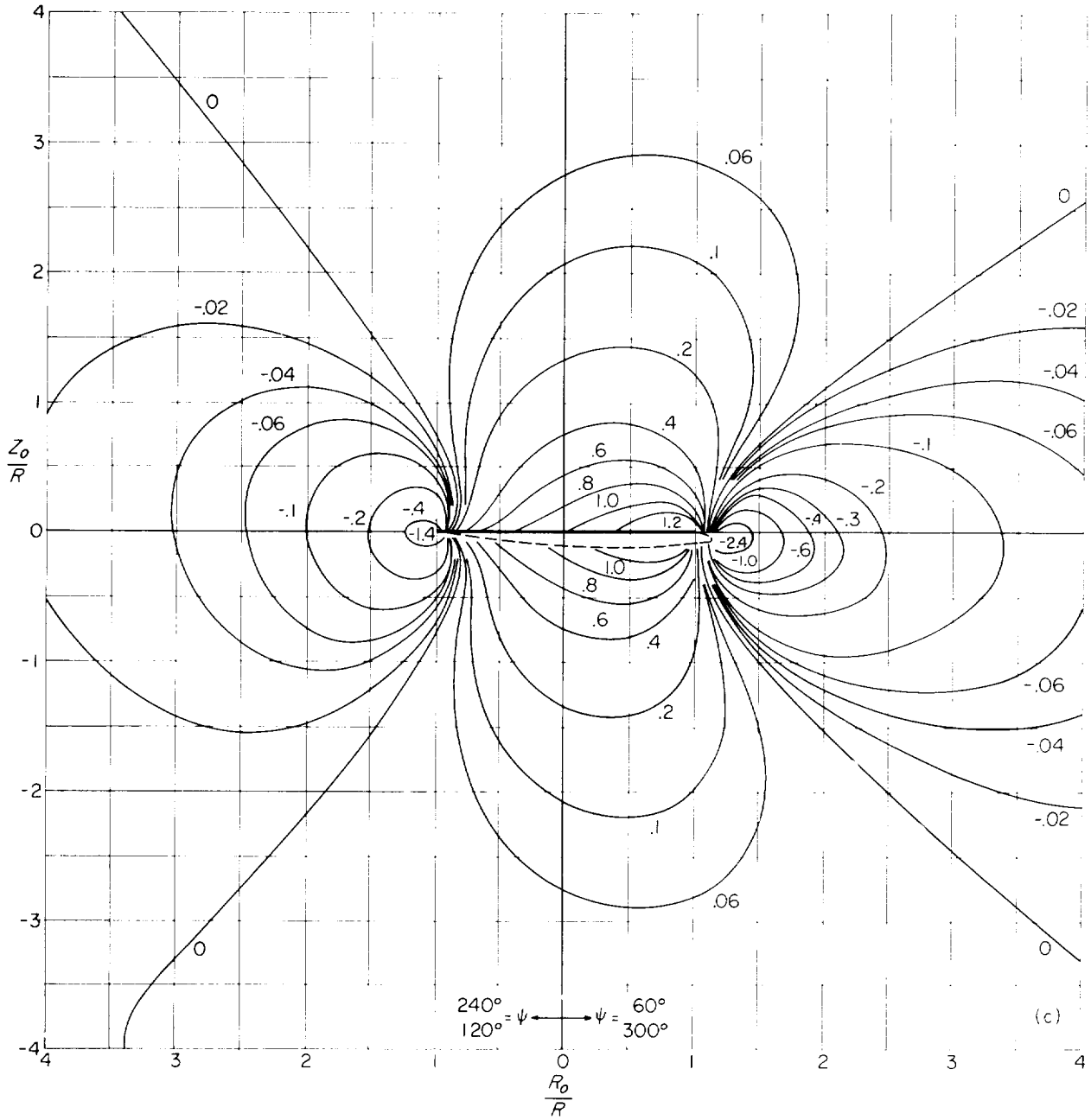

(c) Lines of constant values of V_i/v in azimuth planes $\psi = 60°$ and $240°$ and $\psi = 120°$ and $300°$.

FIGURE 6.— Continued.

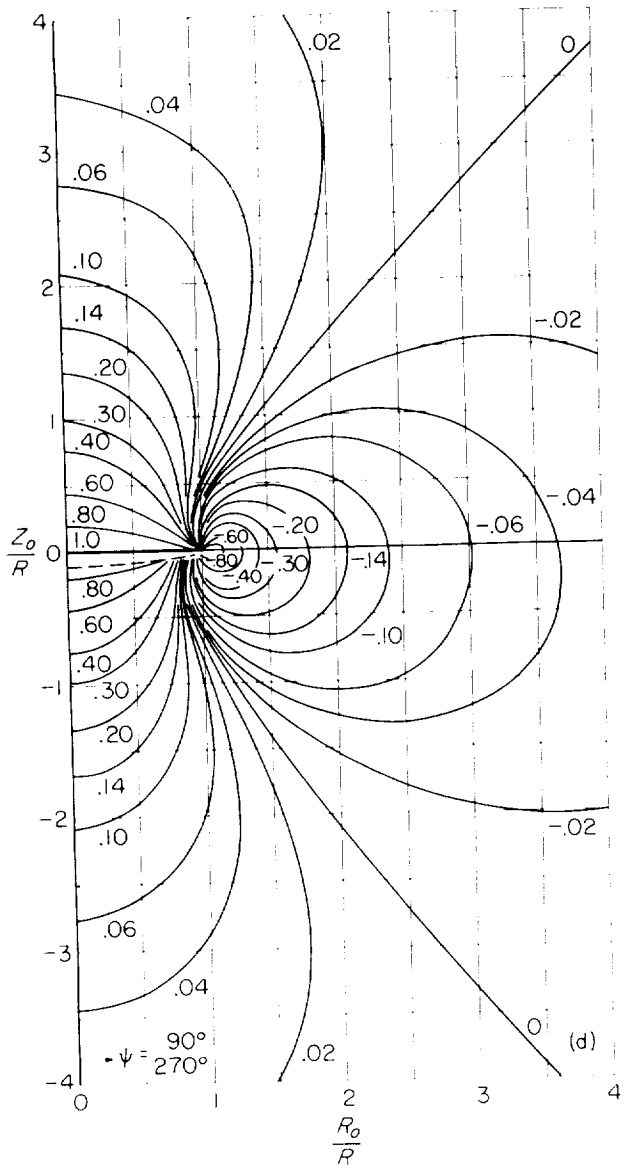

(d) Lines of constant values of V_z/v in lateral plane $\psi = 90°$ and 270°.

FIGURE 6. Concluded.

with those obtained from the experimental values in the lateral plane. The table for these experimental values has not been included since the more accurate computed values were available.

Figures 8(a) to 8(c) give plots of the computed data of table 2. Experimental analog values for the in-plane velocity component are also indicated in these figures for comparison purposes.

In connection with figures 7 and 8, which show comparisons between computed and experimental analog results, it will be noted that no gross differences exist except in regions near the wake boundary wherein neither the uniform mathematical model nor the magnetic analog with its arbitrary finite coil spacing could be expected to yield realistic approximations to the true flow field.

CONCLUDING REMARKS

Inherent in the analog method which has been described are sources of error such as (1) differences in geometry between the model, with its finite arbitrary coil spacing, and the wake-vortex system for a particular rotor, (2) small variations in primary-coil current and frequency, (3) search-coil positioning errors and associated meter-reading errors, (4) inaccuracies in the meter and amplifier calibration, and (5) small distortion in the portion of the model magnetic field of interest arising from the laboratory structure. It is to be expected that the process of fairing the reduced data will average out some of the inaccuracies due to the above causes; however, this need not always be the case. Too, the fairing process itself is subject to varying degrees of inaccuracy depending upon the individual performing the operation. In view of these facts it is difficult to give any figure for the probable range of accuracy of the experimental measurements. However, the comparisons between the calculated and analog results indicate that the experimental values are sufficiently accurate for engineering purposes.

It is anticipated that the computed data presented herein will be useful in synthesizing the distribution of the normal component of induced velocity over the plane of any rotor having a specified loading by some method employing the principle of superposition. Also, it is expected that the data should be useful for estimating the interference-induced velocities of multirotor heli-

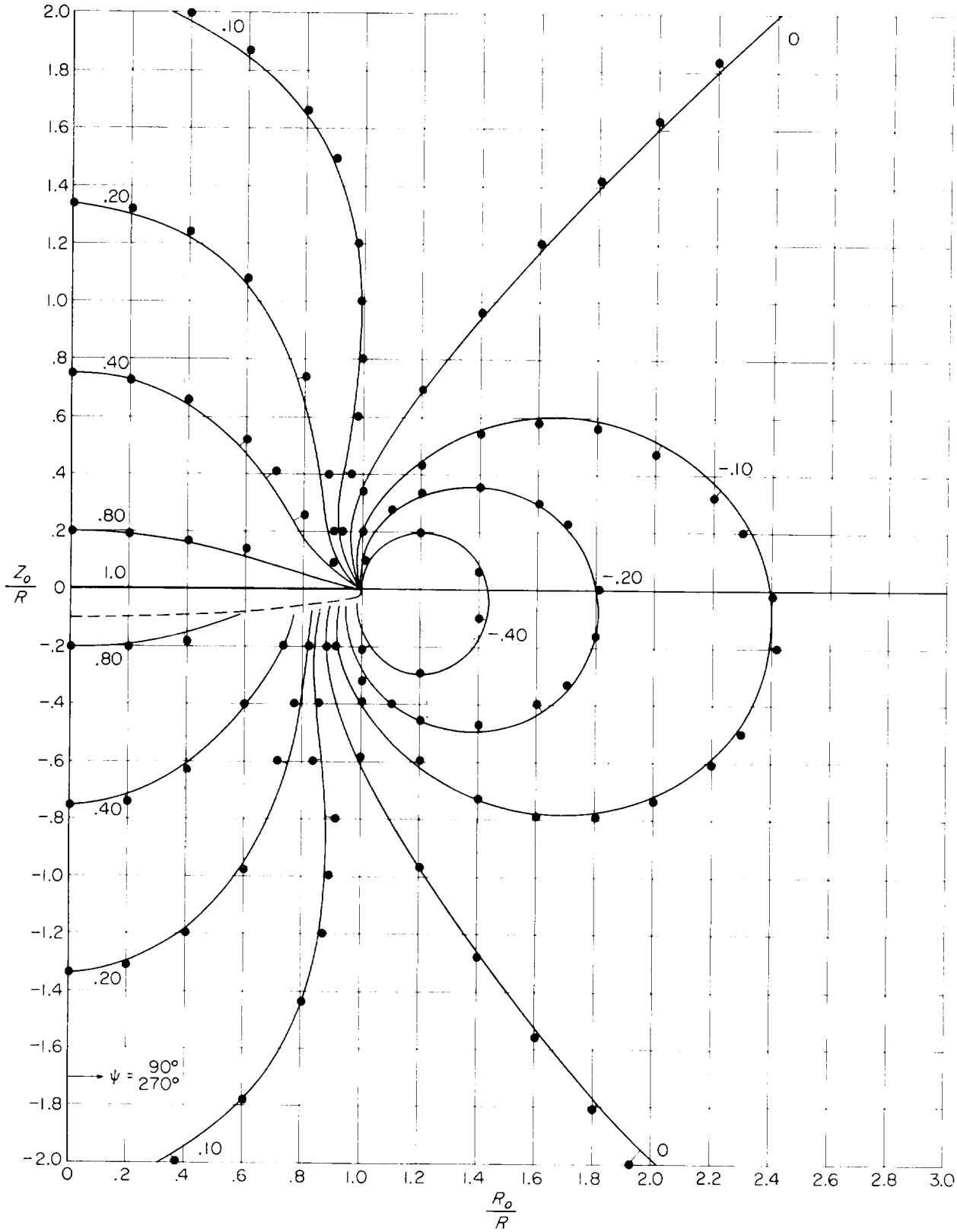

FIGURE 7.—Lines of constant values of V_i/v in lateral plane obtained from computed data of table 1(d) compared with experimental analog values.

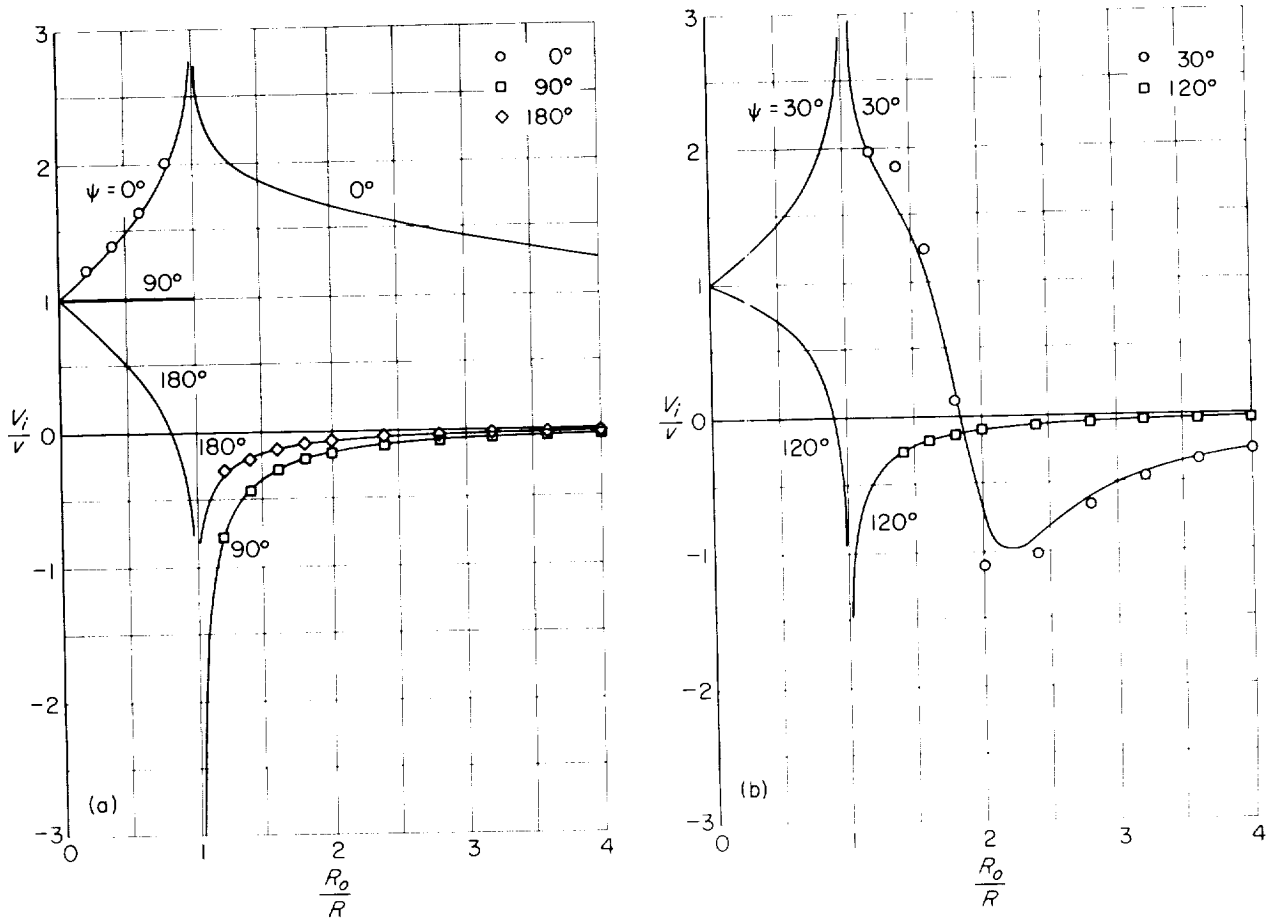

(a) V_i/v in rotor plane for $\psi = 0°$, 90°, and 180°.

(b) V_i/v in rotor plane for $\psi = 30°$ and 120°.

FIGURE 8.—Radial distributions of computed in-plane nondimensional normal component of induced velocity V_i/v at each 30° azimuth position compared with experimental analog values for case of wake angle $\chi = \tan^{-1} 10 = 84.29°$.

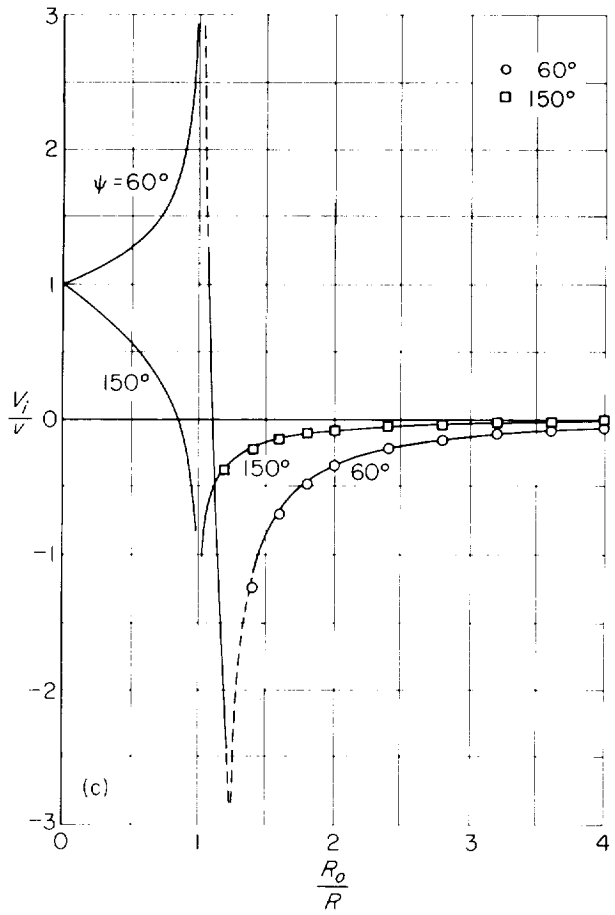

(c) V_i/v in rotor plane for $\psi = 60°$ and 150°.

FIGURE 8.—Concluded.

copters and the downwash velocities at wing and tail planes.

Inasmuch as the apparatus and techniques used in the present work are subject to considerable refinement, it is thought that the electromagnetic-analog method should be useful for mapping induced flow fields which are mathematically intractable.

GEORGIA INSTITUTE OF TECHNOLOGY,
ATLANTA, GA., *February 21, 1957.*

REFERENCES

1. Swanson, Robert S., and Crandall, Stewart M.: An Electromagnetic-Analogy Method of Solving Lifting-Surface-Theory Problems. NACA WR L-120, 1945.
2. Gardner, Clifford S., and LaHatte, James A.: Determination of Induced Velocity in Front of an Inclined Propeller by a Magnetic-Analogy Method. NACA WR L-154, 1946.
3. Castles, Walter, Jr., and De Leeuw, Jacob Henri: The Normal Component of the Induced Velocity in the Vicinity of a Lifting Rotor and Some Examples of Its Application. NACA Rep. 1184, 1954. (Supersedes NACA TN 2912.)
4. Castles, Walter, Jr., and Durham, Howard L., Jr.: Distribution of Normal Component of Induced Velocity in Lateral Plane of a Lifting Rotor. NACA TN 3841, 1956.
5. Heyson, Harry H., and Katzoff, S.: Induced Velocities Near a Lifting Rotor With Nonuniform Disk Loading. NACA Rep. 1319, 1957. (Supersedes NACA TN 3690 and NACA TN 3691.)

TABLE 1.—NONDIMENSIONAL VALUES OF NORMAL COMPONENT OF INDUCED VELOCITY V_i/v IN EACH 30° AZIMUTH PLANE FOR CASE OF WAKE ANGLE $\chi = \text{TAN}^{-1}10 = 84.29°$

(a) V_i/v over azimuth plane $\psi = 0°$

Z_o/R	V_i/v for values of R_o/R of—												
	0	0.2	0.4	0.6	0.8	1.0	1.2	1.4	1.6	1.8	2.0	3.0	4.0
4.0	0.030	0.033	0.036	0.038	0.041	0.043	0.045	0.047	0.048	0.050	0.051	0.055	0.058
3.0	.051	.059	.066	.072	.078	.083	.086	.088	.090	.091	.092	.095	.095
2.0	.106	.122	.137	.151	.164	.176	.186	.194	.200	.203	.204	.191	.183
1.8	.126	.148	.169	.187	.204	.216	.226	.234	.239	.240	.239	.222	.212
1.6	.152	.178	.204	.226	.245	.261	.274	.284	.285	.292	.290	.266	.249
1.4	.186	.222	.254	.282	.305	.323	.337	.346	.350	.348	.341	.314	.296
1.2	.232	.275	.316	.354	.386	.414	.434	.446	.449	.438	.425	.378	.348
1.0	.293	.355	.414	.466	.508	.540	.559	.568	.564	.547	.534	.476	.432
.8	.375	.460	.540	.610	.675	.720	.750	.735	.715	.695	.675	.600	.540
.6	.486	.610	.725	.825	.905	.960	.975	.935	.895	.860	.835	.745	.685
.4	.629	.790	.935	1.075	1.195	1.285	1.255	1.205	1.165	1.125	1.095	.975	.905
.2	.804	1.020	1.250	1.405	1.555	1.675	1.635	1.570	1.520	1.475	1.435	1.280	1.180
0	1.000	1.181	1.377	1.609	1.936		2.072	1.910	1.810	1.737	1.678	1.452	1.270
−.2	.804	1.010	1.240	1.500	1.900								
−.4	.629	.785	.940	1.095	1.250	1.400	1.550	1.690	1.840	1.980	2.12	2.770	
−.6	.486	.600	.710	.825	.935	1.045	1.150	1.260	1.370	1.470	1.575	2.090	2.560
−.8	.375	.445	.520	.595	.665	.735	.810	.880	.950	1.020	1.090	1.425	1.735
−1.0	.293	.355	.420	.480	.540	.600	.655	.710	.765	.815	.865	1.075	1.220
−1.2	.232	.280	.325	.370	.415	.460	.500	.540	.580	.615	.650	.785	.855
−1.4	.186	.220	.255	.290	.320	.355	.385	.415	.445	.470	.495	.600	.655
−1.6	.152	.175	.205	.230	.255	.275	.300	.325	.345	.365	.390	.470	.520
−1.8	.126	.145	.170	.190	.210	.230	.250	.270	.290	.305	.320	.385	.415
−2.0	.106	.120	.140	.155	.170	.185	.205	.220	.230	.245	.260	.305	.325
−3.0	.051	.057	.063	.069	.075	.081	.086	.092	.097	.102	.106	.126	.138
−4.0	.030	.033	.035	.038	.040	.043	.045	.048	.050	.053	.055	.066	.075

TABLE 1.—NONDIMENSIONAL VALUES OF NORMAL COMPONENT OF INDUCED VELOCITY V_i/c IN EACH 30° AZIMUTH PLANE FOR CASE OF WAKE ANGLE $\chi=\text{TAN}^{-1}10=84.29°$ —Continued

(b) V_i/c over azimuth planes $\psi=30°$ and 330°

Z_o/R	V_i/c for values of R_o/R of—															
	0	0.2	0.4	0.6	0.8	1.0	1.2	1.4	1.6	1.8	2.0	2.4	2.8	3.2	3.6	4.0
4.0	0.030	0.032	0.035	0.037	0.039	0.041	0.042	0.044	0.044	0.045	0.045	0.044	0.044	0.040	0.037	0.034
3.6	.037	.040	.044	.047	.050	.052	.054	.056	.058	.058	.058	.057	.053	.049	.043	.037
3.2	.045	.049	.053	.057	.060	.062	.064	.065	.066	.066	.065	.062	.058	.053	.047	.041
2.8	.058	.064	.069	.074	.078	.081	.083	.085	.084	.083	.079	.073	.065	.058	.051	.044
2.4	.077	.087	.094	.101	.106	.110	.111	.111	.110	.107	.103	.090	.079	.068	.057	.046
2.0	.106	.119	.130	.139	.146	.151	.153	.150	.146	.139	.130	.112	.094	.074	.057	.042
1.8	.126	.142	.157	.168	.176	.181	.182	.178	.170	.157	.144	.118	.094	.071	.052	.037
1.6	.152	.174	.193	.206	.215	.218	.216	.209	.197	.180	.163	.130	.098	.071	.048	.030
1.4	.186	.212	.233	.250	.262	.269	.261	.245	.227	.206	.182	.137	.096	.062	.037	.019
1.2	.232	.274	.305	.326	.342	.343	.328	.303	.268	.233	.198	.136	.085	.046	.019	.002
1.0	.293	.345	.391	.428	.433	.418	.394	.360	.314	.264	.214	.127	.064	.020	−.008	−.022
.8	.375	.452	.505	.541	.567	.561	.507	.442	.371	.292	.213	.092	.019	.024	−.043	−.055
.6	.486	.586	.687	.753	.788	.770	.702	.558	.433	.303	.189	.030	−.058	−.094	.104	.103
.4	.629	.760	.885	1.008	1.066	1.066	.950	.700	.460	.270	.105	.120	−.195	−.195	.175	−.154
.2	.804	.960	1.130	1.315	1.530	1.642	1.430	1.080	.600	.215	−.110	−.410	.395	.325	−.260	−.210
0	1.000	1.157	1.332	1.550	1.882	...	1.964	1.580	1.076	.240	.689	−.880	−.603	.426	−.320	.249
−.2	.804	.930	1.101	1.330	1.592	1.780	1.870	1.830	1.370	−.198	2.715	1.222	−.720	−.464	.360	.261
−.4	.629	.745	.895	1.028	1.114	1.140	1.040	.855	.539	−.050	−.464	−.736	.598	−.433	−.329	−.261
−.6	.486	.571	.664	.753	.807	.807	.745	.591	.404	.185	.020	−.314	−.409	.303	−.260	.245
−.8	.375	.446	.530	.581	.608	.608	.555	.461	.358	.226	.094	.109	−.221	−.245	.229	−.199
−1.0	.293	.352	.403	.444	.460	.444	.407	.360	.302	.228	.149	.002	.095	−.140	−.152	−.150
−1.2	.232	.270	.303	.332	.354	.350	.330	.300	.261	.214	.156	.052	.015	.061	−.090	−.104
−1.4	.186	.219	.248	.272	.282	.282	.275	.256	.228	.195	.157	.086	.026	−.021	.052	.069
−1.6	.152	.176	.199	.216	.227	.227	.220	.207	.191	.170	.149	.099	.052	.012	−.017	−.038
−1.8	.126	.144	.162	.176	.186	.190	.186	.178	.167	.154	.138	.102	.066	.033	.005	−.016
−2.0	.106	.124	.139	.150	.157	.160	.160	.156	.150	.141	.131	.104	.075	.048	.023	.002
−2.4	.077	.088	.098	.104	.109	.113	.114	.114	.112	.106	.100	.086	.071	.056	.040	.023
−2.8	.058	.064	.070	.075	.079	.083	.085	.086	.086	.085	.083	.075	.065	.054	.043	.032
−3.2	.045	.050	.054	.058	.062	.064	.067	.068	.069	.069	.069	.064	.057	.050	.043	.035
3.6	.037	.041	.044	.047	.050	.052	.055	.055	.056	.056	.056	.055	.051	.047	.041	.035
4.0	.030	.033	.035	.038	.040	.042	.043	.044	.045	.046	.046	.045	.042	.040	.036	.032

TABLE 1.– NONDIMENSIONAL VALUES OF NORMAL COMPONENT OF INDUCED VELOCITY V_i/v IN EACH 30° AZIMUTH PLANE FOR CASE OF WAKE ANGLE χ TAN $^{-1}10=84.29°$—Continued

(c) V_i/v over azimuth planes $\psi=60°$ and 300°

Z_o/R	V_i/v for values of R_o/R of—															
	0	0.2	0.4	0.6	0.8	1.0	1.2	1.4	1.6	1.8	2.0	2.4	2.8	3.2	3.6	4.0
4.0	0.030	0.031	0.032	0.033	0.033	0.033	0.032	0.031	0.030	0.029	0.027	0.024	0.020	0.016	0.012	0.010
3.6	.037	.038	.039	.040	.041	.041	.040	.039	.037	.036	.032	.027	.021	.016	.012	.009
3.2	.045	.047	.049	.049	.049	.049	.047	.045	.042	.039	.036	.029	.023	.016	.011	.008
2.8	.058	.061	.063	.064	.064	.062	.059	.056	.052	.047	.042	.032	.022	.014	.007	.003
2.4	.077	.081	.084	.085	.083	.079	.075	.069	.062	.054	.046	.031	.019	.009	.002	−.002
2.0	.106	.112	.116	.116	.112	.106	.097	.085	.072	.059	.045	.025	.011	.001	−.006	−.010
1.8	.126	.134	.138	.137	.132	.123	.110	.095	.077	.059	.043	.020	.004	−.007	−.012	−.015
1.6	.152	.159	.167	.163	.154	.141	.122	.100	.079	.058	.039	.011	−.006	−.014	−.018	−.020
1.4	.186	.197	.206	.199	.186	.168	.140	.108	.077	.050	.028	−.001	−.017	−.026	−.028	−.026
1.2	.232	.254	.260	.254	.236	.204	.161	.115	.071	.038	.011	−.020	−.034	−.038	−.038	−.033
1.0	.293	.321	.329	.318	.288	.236	.168	.104	.052	.012	−.016	−.044	−.052	−.050	−.046	−.041
.8	.375	.406	.420	.406	.362	.278	.176	.080	.012	−.032	−.060	−.076	−.072	−.064	−.056	−.049
.6	.486	.532	.546	.536	.474	.348	.174	.024	−.064	−.118	−.120	−.114	−.096	−.080	−.066	−.056
.4	.629	.698	.739	.749	.682	.455	.111	−.138	−.223	−.223	−.204	−.158	−.121	−.095	−.077	−.062
.2	.804	.881	.966	1.060	1.085	.768	−.188	−.531	−.468	−.355	−.285	−.193	−.140	−.106	−.084	−.065
0	1.000	1.091	1.198	1.349	1.635	.....	−2.442	−1.143	−.671	−.457	−.337	−.210	−.146	−.110	−.086	−.066
−.2	.804	.913	1.000	1.050	1.030	.615	−.776	−.912	−.668	−.478	−.359	−.229	−.159	−.118	−.091	−.065
−.4	.629	.704	.740	.740	.650	.335	−.105	−.354	−.376	−.325	−.285	−.206	−.148	−.112	−.088	−.063
−.6	.486	.539	.552	.527	.433	.243	.020	−.154	−.217	−.222	−.205	−.156	−.122	−.095	−.073	−.060
−.8	.375	.406	.416	.389	.330	.206	.086	−.026	−.092	−.124	−.130	−.120	−.099	−.080	−.066	−.056
−1.0	.293	.318	.329	.310	.263	.190	.112	.035	−.026	−.063	.083	−.092	−.084	−.074	−.062	−.051
−1.2	.232	.249	.254	.243	.214	.168	.116	.062	.015	−.018	−.038	−.060	.065	−.060	−.053	−.046
−1.4	.186	.200	.203	.194	.178	.148	.110	.070	.036	.010	−.012	−.036	−.046	−.048	−.044	−.040
−1.6	.152	.163	.167	.160	.148	.128	.104	.077	.051	.026	.008	−.017	−.032	−.036	−.036	−.035
−1.8	.126	.133	.138	.135	.126	.114	.096	.074	.054	.036	.020	−.004	−.019	−.027	−.029	−.029
−2.0	.106	.111	.116	.115	.110	.100	.087	.072	.057	.042	.029	.007	−.009	−.018	−.022	−.023
−2.4	.077	.082	.085	.086	.083	.077	.070	.062	.054	.045	.036	.018	.005	−.005	−.011	−.014
−2.8	.058	.062	.064	.064	.062	.060	.056	.052	.046	.040	.034	.023	.012	.004	−.002	−.006
−3.2	.045	.048	.049	.049	.049	.047	.046	.043	.040	.036	.032	.023	.015	.008	.002	−.001
−3.6	.037	.039	.041	.041	.041	.040	.039	.037	.035	.033	.030	.023	.018	.013	.007	.003
−4.0	.030	.031	.032	.033	.033	.033	.032	.031	.029	.028	.026	.022	.017	.013	.009	.005

TABLE 1.—NONDIMENSIONAL VALUES OF NORMAL COMPONENT OF INDUCED VELOCITY V_i/v IN EACH 30° AZIMUTH PLANE FOR CASE OF WAKE ANGLE $\chi = \text{TAN}^{-1}10 = 84.29°$—Continued

(d) V_i/v over azimuth planes $\psi = 90°$ and 270°

Z_o/R	V_i/v for values of R_o/R of—															
	0	0.2	0.4	0.6	0.8	1.0	1.2	1.4	1.6	1.8	2.0	2.4	2.8	3.2	3.6	4.0
4.0	0.030	0.030	0.030	0.029	0.028	0.026	0.025	0.023	0.021	0.019	0.017	0.012	0.008	0.005	0.003	0.001
3.6	.037	.037	.036	.035	.034	.032	.030	.027	.025	.022	.018	.013	.007	.003	.001	0
3.2	.045	.044	.043	.041	.038	.036	.033	.029	.025	.022	.018	.011	.006	.002	−.001	−.003
2.8	.058	.057	.055	.052	.049	.045	.041	.035	.030	.024	.019	.010	.003	−.001	−.004	−.006
2.4	.077	.076	.074	.069	.063	.056	.049	.041	.033	.024	.017	.006	−.001	−.005	−.007	−.009
2.0	.106	.103	.098	.089	.078	.066	.053	.041	.029	.020	.012	0	−.007	−.010	−.012	−.013
1.8	.126	.123	.116	.104	.089	.073	.056	.041	.027	.016	.007	−.005	−.011	−.014	−.016	−.015
1.6	.152	.148	.138	.121	.102	.080	.058	.039	.023	.010	0	−.012	−.017	−.019	−.019	−.018
1.4	.186	.180	.166	.145	.117	.087	.059	.034	.015	.000	−.010	−.020	−.023	−.023	−.022	−.020
1.2	.232	.226	.205	.173	.134	.093	.055	.024	.015	−.014	−.023	−.030	−.031	−.026	−.024	−.022
1.0	.293	.285	.255	.210	.154	.096	.045	.006	−.019	−.034	−.041	−.042	−.038	−.033	−.029	−.025
.8	.375	.362	.325	.260	.180	.093	.021	−.027	−.052	−.061	−.063	−.056	−.047	−.039	−.033	−.027
.6	.486	.472	.424	.334	.212	.074	−.031	−.083	−.099	−.097	−.089	−.070	−.055	−.043	−.035	−.029
.4	.629	.616	.560	.452	.260	.019	−.142	−.178	−.163	−.138	−.116	−.083	−.062	−.048	−.038	−.031
.2	.804	.794	.758	.658	.432	−.156	−.399	−.314	−.232	−.176	−.140	−.092	−.067	−.050	−.040	−.032
0	1.000	1.000	1.000	1.000	1.000	-----	−.789	−.422	−.277	−.200	−.153	−.099	−.070	−.052	−.042	−.033
−.2	.804	.792	.728	.600	.320	−.461	−.559	−.379	−.265	−.196	−.152	−.099	−.070	−.052	−.042	−.034
−.4	.629	.610	.546	.410	.176	−.120	−.262	−.255	−.211	−.169	−.137	−.094	−.068	−.052	−.042	−.034
−.6	.486	.466	.408	.298	.150	−.008	−.112	−.150	−.148	−.132	−.114	−.084	−.064	−.050	−.041	−.034
−.8	.375	.358	.313	.233	.138	.040	−.036	−.079	−.095	−.095	−.089	−.072	−.057	−.046	−.038	−.033
−1.0	.293	.281	.246	.192	.127	.060	.004	−.034	−.055	−.064	−.066	−.060	−.050	−.042	−.036	−.032
−1.2	.232	.222	.198	.159	.114	.067	.026	−.006	−.028	−.040	−.046	−.047	−.043	−.038	−.034	−.030
−1.4	.186	.181	.162	.136	.103	.068	.037	.011	−.009	−.022	−.030	−.036	−.035	−.033	−.030	−.028
−1.6	.152	.148	.135	.115	.092	.066	.042	.021	.004	−.009	−.017	−.026	−.028	−.028	−.026	−.025
−1.8	.126	.123	.113	.099	.082	.062	.044	.027	.012	.001	−.008	−.018	−.022	−.023	−.023	−.022
−2.0	.106	.103	.097	.086	.072	.058	.043	.029	.017	.007	−.001	−.011	−.017	−.018	−.019	−.020
−2.4	.077	.075	.071	.065	.058	.050	.040	.031	.022	.014	.007	−.003	−.009	−.012	−.014	−.015
−2.8	.058	.057	.054	.051	.046	.041	.035	.028	.022	.017	.012	.003	−.003	−.006	−.009	−.010
−3.2	.045	.044	.043	.041	.038	.034	.030	.026	.022	.018	.014	.007	.001	−.003	−.005	−.006
−3.6	.037	.037	.036	.035	.033	.031	.028	.025	.022	.018	.015	.009	.004	.001	.002	−.004
−4.0	.030	.030	.029	.028	.027	.026	.024	.021	.018	.015	.013	.009	.005	.002	0	−.002

TABLE 1.—NONDIMENSIONAL VALUES OF NORMAL COMPONENT OF INDUCED VELOCITY V_i/v IN EACH 30° AZIMUTH PLANE FOR CASE OF WAKE ANGLE $\chi = \text{TAN}^{-1}10 = 84.29°$—Continued

(e) V_i/v over azimuth planes $\psi = 120°$ and 240°

Z_o/R	V_i/v for values of R_o R of—															
	0	0. 2	0. 4	0. 6	0. 8	1. 0	1. 2	1. 4	1. 6	1. 8	2. 0	2. 4	2. 8	3. 2	3. 6	4. 0
4. 0	0. 030	0. 029	0. 027	0. 025	0. 022	0. 020	0. 017	0. 015	0. 013	0. 011	0. 009	0. 006	0. 003	0. 001	−0. 007	−0. 002
3. 6	. 037	. 035	. 033	. 031	. 028	. 025	. 022	. 019	. 016	. 012	. 009	. 004	. 001	−. 001	−. 002	−. 003
3. 2	. 045	. 042	. 038	. 034	. 030	. 026	. 022	. 018	. 014	. 011	. 008	. 003	0	−. 002	−. 004	−. 005
2. 8	. 058	. 054	. 049	. 043	. 037	. 031	. 024	. 019	. 013	. 009	. 007	. 001	−. 003	−. 005	−. 006	−. 007
2. 4	. 077	. 071	. 063	. 055	. 045	. 036	. 027	. 019	. 012	. 007	. 003	−. 003	−. 007	−. 009	−. 010	−. 010
2. 0	. 106	. 096	. 083	. 068	. 053	. 039	. 027	. 012	. 008	. 002	−. 003	−. 009	−. 012	−. 013	−. 013	−. 013
1. 8	. 126	. 112	. 096	. 077	. 059	. 042	. 027	. 014	. 004	−. 004	−. 008	−. 014	−. 017	−. 017	−. 015	−. 014
1. 6	. 152	. 136	. 115	. 092	. 066	. 042	. 023	. 008	−. 003	−. 010	−. 015	−. 019	−. 020	−. 019	−. 017	−. 016
1. 4	. 186	. 164	. 135	. 102	. 069	. 040	. 017	0	−. 012	−. 019	−. 023	−. 026	−. 025	−. 022	−. 019	−. 017
1. 2	. 232	. 202	. 162	. 122	. 076	. 037	. 010	−. 010	−. 022	−. 030	−. 033	−. 033	−. 029	−. 025	−. 021	−. 018
1. 0	. 293	. 263	. 207	. 147	. 083	. 029	−. 008	−. 031	−. 045	−. 050	−. 051	−. 044	−. 034	−. 028	−. 024	−. 020
. 8	. 375	. 329	. 261	. 169	. 080	. 007	−. 036	−. 061	−. 070	−. 069	−. 064	−. 052	−. 041	−. 033	−. 027	−. 021
. 6	. 486	. 433	. 344	. 212	. 074	−. 035	−. 090	−. 106	−. 102	−. 090	−. 078	−. 058	−. 044	−. 034	−. 028	−. 022
. 4	. 629	. 562	. 450	. 273	. 046	−. 125	−. 183	−. 169	−. 140	−. 111	−. 093	−. 066	−. 049	−. 037	−. 029	−. 023
. 2	.801	.739	.608	.395	.068	−. 389	−. 316	−. 238	−. 175	−. 132	−. 103	−. 070	−. 051	−. 039	−. 030	−. 024
0	1. 000	. 909	. 802	. 651	. 365	-----	−. 451	−. 258	−. 175	−. 129	−. 100	−. 066	−. 047	−. 035	−. 028	−. 023
−. 2	. 804	. 679	. 552	. 297	. 048	−. 321	−. 300	−. 212	−. 154	−. 114	−. 088	−. 058	−. 041	−. 030	−. 024	−. 022
−. 4	. 629	. 533	. 409	. 222	. 019	−. 125	−. 173	−. 156	−. 128	−. 102	−. 084	−. 057	−. 041	−. 031	−. 024	−. 021
−. 6	. 486	. 409	. 300	. 179	. 057	−. 040	−. 088	−. 098	−. 094	−. 084	−. 071	−. 052	−. 039	−. 029	−. 023	−. 020
−. 8	. 375	. 306	. 235	. 150	. 065	−. 001	−. 041	−. 061	−. 066	−. 063	−. 057	−. 045	−. 034	−. 028	−. 022	−. 018
−1. 0	. 293	. 244	. 190	. 128	. 072	. 022	−. 012	−. 032	−. 040	−. 044	−. 044	−. 038	−. 030	−. 024	−. 020	−. 017
−1. 2	. 232	. 205	. 160	. 115	. 069	. 035	. 007	−. 012	−. 023	−. 028	−. 031	−. 031	−. 026	. 022	−. 018	−. 016
−1. 4	. 186	. 163	. 132	. 098	. 067	. 040	. 018	0	−. 012	−. 018	−. 022	−. 024	−. 022	−. 019	−. 017	−. 015
−1. 6	. 152	. 136	. 113	. 087	. 063	. 041	. 022	. 008	−. 003	−. 010	−. 015	−. 019	−. 018	−. 016	−. 014	−. 013
−1. 8	. 126	. 112	. 096	. 076	. 058	. 041	. 026	. 014	. 004	−. 003	−. 008	−. 013	−. 015	−. 014	−. 013	−. 012
−2. 0	. 106	. 096	. 082	. 067	. 054	. 039	. 031	. 016	. 007	. 001	−. 004	−. 010	−. 013	−. 013	−. 011	−. 011
−2. 4	. 077	. 070	. 064	. 055	. 046	. 036	. 027	. 019	. 013	. 008	. 004	−. 004	−. 007	−. 009	−. 009	−. 008
−2. 8	. 058	. 054	. 049	. 043	. 037	. 030	. 024	. 019	. 014	. 010	. 006	. 001	−. 002	−. 004	−. 005	−. 006
−3. 2	. 045	. 042	. 039	. 035	. 031	. 027	. 023	. 019	. 015	. 011	. 008	. 004	. 001	−. 002	−. 003	−. 004
−3. 6	. 037	. 035	. 033	. 030	. 027	. 024	. 021	. 018	. 015	. 012	. 009	. 005	. 003	. 001	−. 001	−. 002
−4. 0	. 030	. 028	. 026	. 025	. 022	. 020	. 018	. 016	. 014	. 011	. 009	. 006	. 003	. 001	−. 001	−. 001

TABLE 1.—NONDIMENSIONAL VALUES OF NORMAL COMPONENT OF INDUCED VELOCITY V_i/v IN EACH 30° AZIMUTH PLANE FOR CASE OF WAKE ANGLE $\chi = \text{TAN}^{-1}10 = 84.29°$—Continued

(f) V_i/v over azimuth planes $\psi = 150°$ and 210°

Z_o/R	V_i/v for values of R_o/R of—															
	0	0. 2	0. 4	0. 6	0. 8	1. 0	1. 2	1. 4	1. 6	1. 8	2. 0	2. 4	2. 8	3. 2	3. 6	4. 0
4. 0	0. 030	0. 028	0. 026	0. 023	0. 021	0. 018	0. 015	0. 013	0. 011	0. 009	0. 007	0. 004	0. 002	0	−0. 001	−0. 002
3. 6	. 037	. 033	. 030	. 026	. 023	. 019	. 016	. 013	. 011	. 008	. 006	. 003	0	−. 002	−. 003	−. 004
3. 2	. 045	. 040	. 035	. 031	. 026	. 022	. 017	. 014	. 010	. 007	. 006	. 002	−. 001	−. 004	−. 004	−. 005
2. 8	. 058	. 051	. 044	. 038	. 031	. 025	. 020	. 014	. 010	. 006	. 003	−. 001	−. 004	−. 006	−. 006	−. 007
2. 4	. 077	. 067	. 056	. 046	. 037	. 028	. 020	. 013	. 008	. 003	. 001	−. 005	−. 007	−. 008	−. 009	−. 009
2. 0	. 106	. 089	. 073	. 058	. 043	. 030	. 019	. 010	. 004	−. 002	−. 006	−. 010	−. 012	−. 012	−. 012	−. 011
1. 8	. 126	. 104	. 083	. 063	. 045	. 031	. 017	. 007	−. 001	−. 007	−. 011	−. 015	−. 015	−. 014	−. 013	−. 012
1. 6	. 152	. 124	. 097	. 073	. 050	. 030	. 014	. 002	. 007	−. 012	−. 015	−. 019	−. 019	−. 016	−. 015	−. 013
1. 4	. 186	. 149	. 114	. 081	. 051	. 027	. 008	−. 006	−. 014	−. 019	−. 022	−. 023	−. 022	−. 018	−. 017	−. 014
1. 2	. 232	. 186	. 137	. 091	. 052	. 021	−. 002	−. 016	−. 024	−. 028	−. 030	−. 029	−. 025	−. 021	−. 018	−. 015
1. 0	. 293	. 226	. 161	. 104	. 052	. 009	−. 018	−. 034	−. 040	−. 042	−. 040	−. 034	−. 028	−. 024	−. 020	−. 016
. 8	. 375	. 288	. 194	. 112	. 044	−. 011	−. 041	−. 056	−. 058	−. 054	−. 048	−. 044	−. 032	−. 027	−. 022	−. 017
. 6	. 486	. 374	. 254	. 132	. 032	−. 046	−. 080	−. 086	−. 082	−. 072	. 060	−. 046	−. 035	−. 029	−. 023	−. 018
. 4	. 629	. 488	. 336	. 166	0	−. 113	−. 144	−. 128	. 104	−. 083	−. 069	. 050	−. 038	−. 030	−. 024	−. 019
. 2	. 804	. 640	. 458	. 232	−. 056	−. 285	−. 248	−. 178	−. 150	−. 098	−. 077	−. 053	−. 038	. 030	−. 024	−. 019
0	1. 000	. 843	. 668	. 450	. 118		−. 344	−. 201	−. 138	. 102	. 079	−. 053	−. 038	−. 028	. 022	−. 018
−. 2	. 804	. 624	. 424	. 184	−. 100	−. 313	−. 252	−. 162	. 122	−. 090	−. 070	. 056	−. 032	−. 024	−. 019	−. 017
−. 4	. 629	. 480	. 310	. 130	−. 028	−. 124	−. 152	−. 124	−. 094	−. 074	−. 060	−. 043	. 032	. 024	−. 019	−. 016
−. 6	. 486	. 368	. 234	. 108	. 010	−. 056	−. 086	−. 090	−. 080	−. 066	. 056	−. 040	−. 030	−. 024	−. 018	−. 015
−. 8	. 375	. 288	. 192	. 104	. 034	−. 018	−. 047	−. 057	−. 058	−. 054	−. 048	. 038	−. 029	−. 023	−. 018	−. 014
−1. 0	. 293	. 220	. 152	. 092	. 042	. 004	. 020	−. 034	−. 040	−. 040	−. 036	−. 030	. 024	−. 020	−. 016	−. 013
−1. 2	. 232	. 188	. 127	. 083	. 046	. 012	−. 006	. 020	−. 026	−. 028	. 029	−. 026	−. 022	−. 018	−. 015	−. 012
−1. 4	. 186	. 147	. 109	. 076	. 048	. 023	. 004	−. 008	. 016	−. 020	−. 020	. 022	−. 020	−. 017	−. 014	−. 011
−1. 6	. 152	. 122	. 094	. 068	. 046	. 026	. 011	. 001	. 007	−. 012	−. 015	−. 017	−. 016	−. 014	−. 012	−. 010
−1. 8	. 126	. 103	. 081	. 061	. 044	. 029	. 016	. 006	−. 002	. 007	. 011	−. 015	. 015	−. 013	. 011	−. 010
−2. 0	. 106	. 087	. 068	. 052	. 039	. 027	. 018	. 009	. 004	−. 003	. 006	−. 010	−. 012	−. 011	−. 010	−. 009
−2. 4	. 077	. 066	. 055	. 045	. 035	. 027	. 019	. 013	. 007	. 003	−. 001	−. 006	−. 008	. 008	−. 008	−. 007
−2. 8	. 058	. 051	. 044	. 037	. 030	. 024	. 019	. 014	. 010	. 006	. 003	. 002	−. 004	−. 005	−. 006	−. 006
−3. 2	. 045	. 040	. 035	. 031	. 026	. 022	. 018	. 014	. 010	. 008	. 005	. 002	. 001	−. 003	−. 004	−. 004
−3. 6	. 037	. 033	. 030	. 026	. 023	. 019	. 016	. 014	. 011	. 009	. 007	. 003	. 001	−. 001	−. 002	−. 003
−4. 0	. 030	. 027	. 025	. 022	. 020	. 017	. 015	. 012	. 010	. 008	. 006	. 003	. 001	−. 001	. 002	−. 002

TABLE 1.—NONDIMENSIONAL VALUES OF NORMAL COMPONENT OF INDUCED VELOCITY V_i/v IN EACH 30° AZIMUTH PLANE FOR CASE OF WAKE ANGLE $\chi = \tan^{-1}10 = 84.29°$—Concluded

(g) V_i/v over azimuth plane $\psi = 180°$

Z_o/R	V_i/v for values of R_o/R of—												
	0	0.2	0.4	0.6	0.8	1.0	1.2	1.4	1.6	1.8	2.0	3.0	4.0
4.0	0.030	0.027	0.024	0.022	0.019	0.017	0.014	0.012	0.010	0.009	0.007	0.002	−0.001
3.0	.051	.044	.038	.032	.026	.022	.018	.014	.011	.008	.006	−.002	−.003
2.0	.106	.088	.070	.055	.041	.030	.020	.012	.005	0	−.003	−.009	.008
1.8	.126	.102	.080	.061	.044	.030	.019	.009	.002	−.035	−.007	−.011	−.009
1.6	.152	.120	.091	.067	.046	.029	.015	.045	−.003	−.008	−.011	−.013	−.010
1.4	.186	.145	.109	.078	.051	.028	.009	−.003	−.010	−.015	−.018	−.016	−.011
1.2	.232	.176	.128	.086	.050	.021	0	−.014	−.021	−.024	−.025	−.018	−.012
1.0	.293	.218	.154	.098	.050	.012	−.015	−.030	−.037	−.038	−.037	−.021	−.013
.8	.375	.268	.180	.106	.044	−.008	−.040	−.051	−.051	−.047	−.044	−.024	−.013
.6	.486	.356	.234	.126	.028	−.042	−.074	−.084	−.076	−.064	−.054	.025	−.014
.4	.629	.448	.288	.140	.008	−.104	−.133	−.128	−.096	−.075	−.062	−.026	−.015
.2	.804	.620	.425	.210	−.050	−.270	−.215	−.155	−.120	−.090	−.070	.027	−.015
0	1.000	.819	.623	.391	.064		−.316	−.186	−.128	−.095	−.074	−.030	−.017
−.2	.804	.617	.385	.149	−.095	−.279	−.221	−.155	−.114	−.084	−.069	−.030	−.016
−.4	.629	.475	.285	.105	.022	−.105	−.135	−.115	−.095	−.080	−.065	−.030	−.016
−.6	.486	.369	.225	.104	.015	−.049	−.074	−.078	−.075	−.066	−.052	−.027	−.016
−.8	.375	.284	.185	.100	.032	−.012	−.038	−.050	−.051	−.049	−.044	−.025	−.015
−1.0	.293	.218	.151	.092	.041	.006	−.017	−.029	−.034	−.036	−.037	−.022	−.014
−1.2	.232	.175	.124	.082	.045	.017	−.002	−.014	−.021	−.026	−.028	−.021	−.013
−1.4	.186	.141	.110	.072	.047	.025	.010	.002	−.011	−.017	−.022	−.017	−.012
−1.6	.152	.127	.089	.063	.045	.027	.014	.003	−.005	−.010	−.014	−.015	−.011
−1.8	.126	.101	.089	.061	.044	.030	.017	.006	−.001	−.006	−.009	−.012	−.010
−2.0	.106	.085	.066	.051	.039	.028	.019	.011	.005	−.001	−.005	−.011	−.009
−3.0	.051	.044	.037	.032	.026	.021	.017	.013	.010	.007	.005	−.003	−.004
−4.0	.030	.027	.024	.022	.019	.017	.014	.012	.010	.008	.006	.001	.001

TABLE 2.—NONDIMENSIONAL VALUES OF NORMAL COMPONENT OF INDUCED VELOCITY V_i/v IN PLANE OF LIFTING ROTOR FOR WHICH $\chi = \tan^{-1}10 = 84.29°$

R_w/R	V_i/v for values of ψ of						
	0°	30°	60°	90°	120°	150°	180°
0	1.000	1.000	1.000	1.000	1.000	1.000	1.000
.2	1.181	1.157	1.091	1.000	.909	.843	.819
.4	1.377	1.332	1.198	1.000	.802	.668	.623
.6	1.609	1.550	1.349	1.000	.651	.450	.391
.8	1.936	1.882	1.635	1.000	.365	.118	.064
.9	2.215	2.187	1.978	1.000	.023	−.187	−.215
.94	2.402	2.398	2.264	1.000	−.264	−.398	−.402
.98	2.774	2.828	2.935	1.000	−.935	−.828	−.774
1.02	2.725	----	----	−3.801	−1.483	−1.024	−.829
1.06	2.400	2.942	1.325	−1.911	−.924	−.670	−.608
1.1	2.262	2.366	.127	−1.352	−.706	−.524	−.478
1.2	2.072	1.964	−2.442	−.790	−.451	−.344	−.316
1.4	1.910	1.580	−1.143	−.423	−.258	−.201	−.186
1.6	1.810	1.076	−.671	−.278	−.175	−.138	−.128
1.8	1.737	.240	−.457	−.201	−.129	−.102	−.095
2.0	1.678	−.689	−.337	−.154	−.100	.079	.074
2.2	1.626	−.977	−.261	−.122	−.080	.064	.059
2.4	1.578	−.880	.210	−.100	−.066	.053	.049
2.6	1.533	.730	.173	−.083	.055	.044	.041
2.8	1.492	.603	−.146	.071	.047	.038	.035
3.0	1.452	.504	.124	.061	.040	.033	.030
3.5	1.357	.342	.088	.044	.029	.024	−.022
4.0	1.270	.249	.066	−.033	.023	.018	.017
4.5	1.189	.190	.052	.026	.018	.014	.013
5.0	1.113	.150	−.042	.021	.014	.012	.011
5.5	1.041	.122	.034	.018	.012	.010	.009
6.0	.975	.102	.029	.015	.010	.008	.008

U.S. GOVERNMENT PRINTING OFFICE: 1960